Available online at www.sciencedirect.com

SCIENCE DIRECT®

Catalysis Today 104 (2005) 114–119

CATALYSIS TODAY

www.elsevier.com/locate/cattod

Mechanosynthesis of complex oxides and preparation of mixed conducting nanocomposites for catalytic membrane reactors

V.V. Zyryanov[a,*], N.F. Uvarov[a], V.A. Sadykov[b], Y.V. Frolova[b], G.M. Alikina[b], A.I. Lukashevich[b], M.I. Ivanovskaya[c], J.M. Criado[d], S. Neophytides[e]

[a] Institute of Solid State Chemistry SB RAS, Novosibirsk, Russia
[b] Boreskov Institute of Catalysis SB RAS, Novosibirsk, Russia
[c] Research Institute for Physical Chemical Problems of the Belarus State University, Minsk, Belarus
[d] Institute de Ciencias de Materiales, Sevilla, Spain
[e] Institute of Chemical Engineering and High Temperature Processes, Patras, Greece

Abstract

Nanopowders of $LaGaO_3$- and $LaMnO_3$-based complex perovskites (P) and ceria-based fluorites (F) were prepared by mechanosynthesis. Compatible nanocomposites F + P and P + P with mixed ion and electron conducting (MIEC) properties were prepared and sintered at moderate temperatures up to dense ceramics. The obtained materials were studied by means of XRD, SEM, TEM, electrical conductivity measurements, temperature programmed (TP) reduction/oxidation and preliminary estimations of permeability were obtained. A new strategy based on the advantages of the mechanochemical ceramic approach is proposed to design multilayer ceramic membranes for CMR. Casting technology and one-step sintering were used for the production of thin film membranes with MIEC properties on porous substrates. The coarse fraction of as-milled powders from agglomerates with density ~70% was used for the porous substrate, and fine fractions of aggregates with sizes <1 μm were used in preparation of composites for thin dense films. Ceria-based composites prepared by the Pechini route and/or mechanochemical method are proposed as materials for protecting thin films.

Keywords: Mechanosynthesis; Nanopowders; Mixed oxides; Perovskites; Fluorites; Composites; Mixed ionic electronic conductors (MIEC); Catalytic membrane reactors (CMR); Methane conversion

1. Introduction

Catalytic membrane reactors (CMR) offer the possibility of producing synthesis gas from methane and air while avoiding the need for either initial separation of the oxygen from the air or post-separation of the nitrogen from the synthesis gas. The high reaction temperature requires the use of a ceramic membrane which has adequate oxygen permeability and which remains stable for a long time. The ideal solution is to deposit a thin film of the membrane onto a porous substrate. This gives the highest permeation possible from the material, due to its small thickness. Dense oxide ceramic membranes with mixed ionic and electronic conductivity (MIEC) have been extensively studied because of their promising applications for oxygen separation, syngas production and oxidative coupling of methane [1–5]. A number of modern techniques are used for mixed oxide powders synthesis and dense ceramics production [6]. However, membrane reactors suitable for commercial applications with high durability have not yet been created. The application of mixed-conducting membranes is limited by some disadvantages of existing membrane materials. Thus, $La_{0.7}Sr_{0.3}Ga_{0.6}Fe_{0.4}O_{3-\delta}$ perovskite possessing the highest oxygen mobility at elevated (750–1000 °C) temperatures [7] is rather expensive and exhibits a high reactivity towards CO_2 and CH_4 leading to degradation of its performance with time. Fluorite-related Pr-doped CeO_2 as well as $SrFeO_3$-based perovskites possesses poor mechanical properties. Another group of membrane materials called

---

* Corresponding author. Fax: +7 3833 322847.
E-mail address: vladi@mail.nsk.ru (V.V. Zyryanov).

0920-5861/$ – see front matter © 2005 Elsevier B.V. All rights reserved.
doi:10.1016/j.cattod.2005.03.047

the dual-phase composites is comprised of the mixture of an oxide ionic conductor and an electronically conducting phase [7–14]. For the composite mixed conductor, it is possible to choose good ionic and electronic conductors as components, and to control the mixed conductivity by adjusting the fraction of constituents. Composites based on CeO_2 are considered to be the most promising. Gd-doped CeO_2 is a well-known oxygen-conducting electrolyte recently receiving much attention as a model material to investigate nano-scale effects in conductivity [15–16]. The preparation of composites from commercially available fine powders usually requires long time ball milling for better mixing of the components. Direct preparation of nanocomposites is possible by the Pechini process [17], but in this case the choice of promising systems is limited. The aim of this work is the synthesis of new materials and the development of planar mixed conducting multilayer membranes which can be used in reactors for efficient methane conversion into syngas. The use of bilayer membranes with protective film was proposed in [18]. Planar membranes may be easily produced by conventional casting technology. A small modification of such an approach will allow using it for the multilayer tubular membranes fabrication which is promising for up-scaling. A new strategy for the design of catalytic membranes with high oxygen permeability is based on the application of the mechanochemical approach (MA) for obtaining nanosize powders and composites with a specific morphology. This technique allows superfast synthesis of mixed oxides – complex perovskites and fluorites with a high conductivity in high energy planetary mills [10,19,20].

2. Experimental

For the preparation of single-phase powders with fluorite or perovskite structure, mixtures of oxides were milled in a high energy planetary mill AGO-2 for 20–30 min. The mass of chromium steel balls (10 mm diameter) loaded into the drum was 220 g, while the starting mass of powder mixtures was about 15 g. For monitoring the process of mechanosynthesis by X-ray diffraction (XRD) analysis, 2–3 probes of a product were taken during milling. A special procedure of the mechanical treatment was used to decrease drastically the contamination of the powders by iron, to increase the ball milling efficiency, and to enhance their phase and size uniformity [21].

For preparation of the composites, single-phase fine fractions of strongly aggregated powders were mixed for 6 min in a planetary micro-mill with one milling body in the form of a hexagonal prism made from the WC/Co alloy. These mixtures were then uniaxially pressed at 100 MPa into disk-shaped pellets. The green density of the as-pressed pellets was within 60–65% of the theoretical density. For comparison, pressing of powders obtained by the Pechini process in the same conditions gives a green density of the pellets within 35–40%. The pellets were sintered at temperatures in the range of $1373 \leq T_s \leq 1523$ K for 6 min. The density of each sintered pellet was determined by the Archimedes method.

Phase characterization was carried out by XRD using Cu Kα radiation. The data were collected in the 2Θ range 10–80° with a step 0.01, peaks being approximated by the Lorenzian shape. The X-ray particle size was estimated using the Scherrer equation.

The total electric conductivity of samples was measured in air at temperatures ranging from 300 to 1000 K using a 4284 A Precision LCR Meter. Measurements were carried out either in the isothermal or heating-cooling mode with a temperature ramp of 3 K/min. Two silver paste electrodes were used as electrical probes.

EM images were recorded by a Tesla BS-350 SEM and a JEOL JEM-2010 TEM operating at 200 kV.

To estimate the lattice oxygen mobility of the nanocomposites in dynamic conditions following earlier described procedures [22], sample reduction by CH_4 (1% in He, CH_4 TPR), reoxidation by O_2 (1% O_2 in air, O_2 TPO) and O_2 desorption into a stream of He (O_2 TPD) in a temperature-programmed (TP) mode (temperature ramp 5 grad/min from 25 up to 880 °C) have been carried out in a flow installation equipped with an IR absorbance gas analyzer PEM-2M and an electrochemical H_2 detector with data acquisition and processing through a PC. For these experiments, sintered pellets were crushed and thoroughly pounded with the pestle up to micron sizes (the specific surface area of those powders was found to be $\sim$1 m^2/g). The powders were then pressed into pellets, crushed and sieved to obtain the 0.5–1 mm fraction to be loaded into a reactor. Before temperature programmed reduction (TPR) and temperature programmed desorption (TPD), samples were pretreated in O_2 at 500 °C or in simulated air at 880 C, respectively. The temperature programmed oxidation (TPO) was carried out after a CH_4 TPR run followed by pretreatment in He for 1 h at 500 C.

Planar multilayered membranes in the form of disks with a diameter of 15 mm were fabricated by casting slurries with different compositions. The slurries were prepared based on ethanol with addition of polyvinylbutyral. The electro-mass-classifier technique (EMC) was used for the separation of powders as milled in fractions [23]. The powder fraction with large (20–100 μm) agglomerates was used for creating the porous support. The superfine (<1 μm) fractions of aggregates were used for the fabrication of dense fine grain ceramics and composites.

3. Results and discussion

The mechanosynthesis of mixed oxides is a well-known approach [24], but technical problems related to its application such as product contamination by milling bodies, agglomeration of ceramic powders and technology up-scaling were solved only recently [21,25] and a semiquantitative theory of this complex process was developed [26]. According to this theory, the chemical interaction on contacts between solid particles in primary acts of mechanical loading gets through formation of atomic mixture by the roller mass transfer – so called the transient dynamic state (D)*. The relaxation of this dynamic state in conditions of quenching and decompression leads to formation of products supersaturated by vacancies. Binary oxides derived by mechanosynthesis are metastable disordered solid solutions undergoing, as a rule, phase transformations at moderate temperatures [19]. Kinetic stabilization of the mixed oxides with cubic perovskite and fluorite structures was achieved by their complex doping thus forming multicomponent solid solutions [20]. Such a complex doping is required as well for obtaining compatible phases in composites. Dense ceramics comprised of complex fluorites and perovskites derived by mechanosynthesis were shown to sinter at relatively low temperatures [10,20,22]. The high sintering activity of nanopowders derived by mechanochemical activation or mechanosynthesis is related to the specific morphology of the powders (Fig. 1). According to the data of mercury porosimetry and helium pycnometry [25], the density of agglomerates with sizes of 2–100 μm (formed by packing of aggregates) is ~70%, while that of aggregates (sizes <1 μm) is ~80%, and the density of disordered crystallites with sizes of 5–50 nm is ~91–99% of the theoretical value. Such morphology of nanopowders provides simultaneously a high green density and a high sintering activity due to the supersaturation by vacancies.

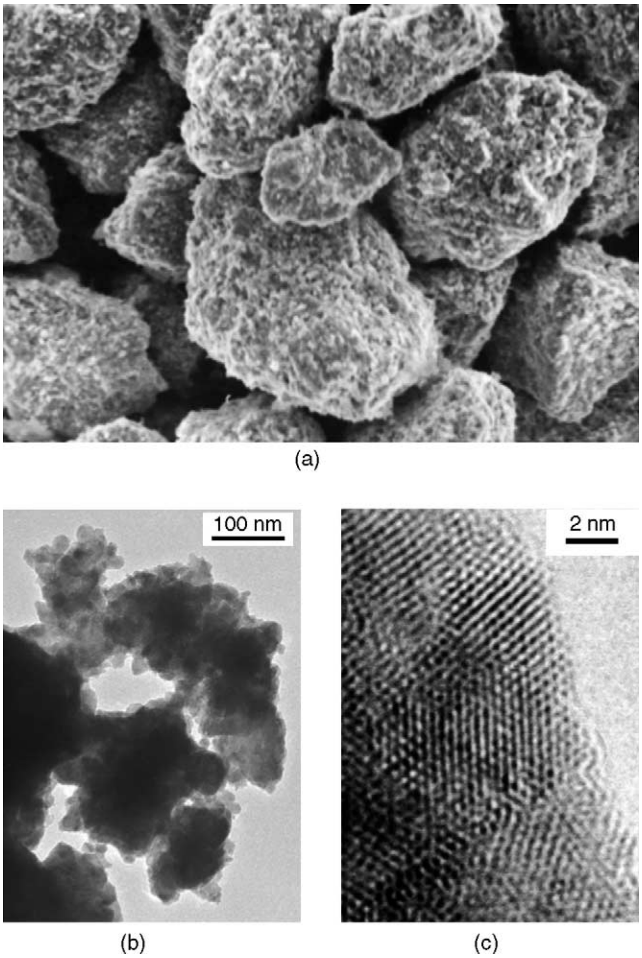

Fig. 1. Typical SEM images of agglomerates 20–100 μm (a) and aggregates <1 μm (b), TEM image (c) of crystallites with domains, twin boundaries for $Bi_{1.5}Y_{0.3}Sm_{0.2}O_{3+x}$, derived by mechanosynthesis.

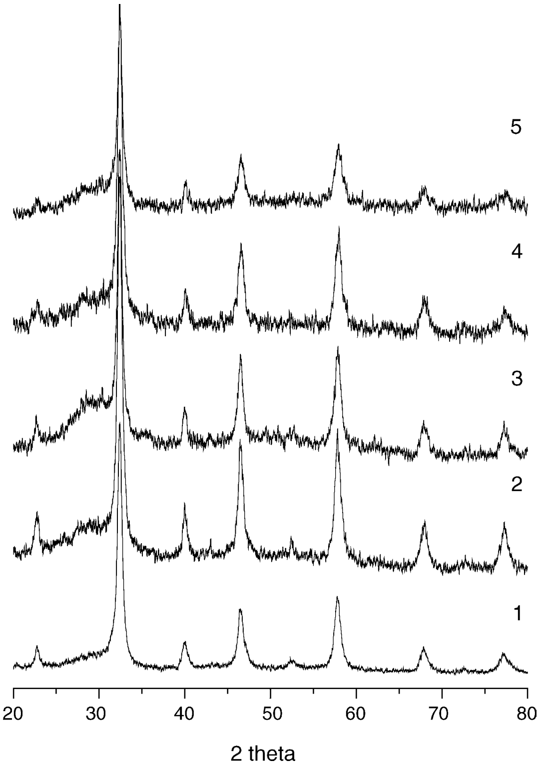

Fig. 2. XRD patterns of $LaGaO_3$-based perovskites as received by mechanosynthesis: (1) $La_{0.8}Sr_{0.2}Ga_{0.8}Mg_{0.2}O_{2.8}$; (2) $La_{0.7}Sr_{0.2}Bi_{0.1}Ga_{0.7}Mg_{0.2}Fe_{0.1}O_{2.8}$; (3) $La_{0.6}Sr_{0.2}Ca_{0.1}Bi_{0.1}Ga_{0.6}Mg_{0.1}Zn_{0.1}Fe_{0.2}O_{2.75}$; (4) $La_{0.6}Sr_{0.2}Ca_{0.1}Bi_{0.1}Ga_{0.6}Mg_{0.1}Zn_{0.1}Fe_{0.1}Co_{0.1}O_{2.75}$; (5) $La_{0.6}Sr_{0.15}Ca_{0.15}Bi_{0.1}Ga_{0.55}Mg_{0.1}Zn_{0.05}Zr_{0.05}Al_{0.05}Fe_{0.1}Co_{0.1}O_{2.75}$.

Typical XRD patterns of $LaGaO_3$-based perovskites as received by mechanosynthesis and after sintering are shown in Figs. 2 and 3. After sintering, the amount of impurity phases is less than 5% and decreases with increasing the milling time, *T*, and the time of sintering. The X-ray size of the crystallites in powders as-prepared by mechanosynthesis are in the range of 20–40 nm.

A sintering of composites leads to inevitable chemical interaction between components (interdiffusion). The most promising composites with a relatively low interdiffusion are based on ceria solid solutions [8] and all-perovskite systems [10,22]. Components with a high oxygen ion conductivity among all-perovskite composites are based on doped $LaGaO_3$. As an electron conducting component, $LaMnO_3$-based solid solutions can be used. Complex perovskites, such as $La_{0.4}Ca_{0.4}Bi_{0.2}Mn_{0.6}Fe_{0.4}O_{3-x}$, can be used for the support production where Bi is introduced for lowering the temperature of sintering and increasing

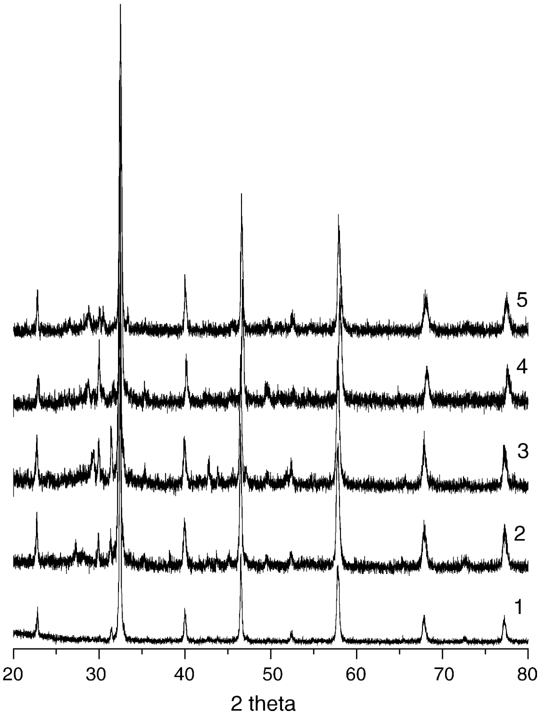

Fig. 3. XRD patterns of $LaGaO_3$-based perovskites after sintering up to dense ceramics.

the exchange reaction, Ca instead of Sr for decreasing the chemical reactivity towards CO_2, Fe for increasing the oxygen conductivity, improving the compatibility in thermal expansion and matching shrinkage levels during sintering by covering dense thin layers. An interdiffusion leads to changes in the lattice parameters of the initial constituents during the sintering of dense ceramics (cf. Fig. 4). Unit cell parameters of individual cubic perovskites derived by the mechanosynthesis are 38,873(13) and 38,585(15) Å. After sintering of composites with a mass ratio of 1:1, the unit cell parameters become 38,764(21) and 38,644(51) Å accordingly.

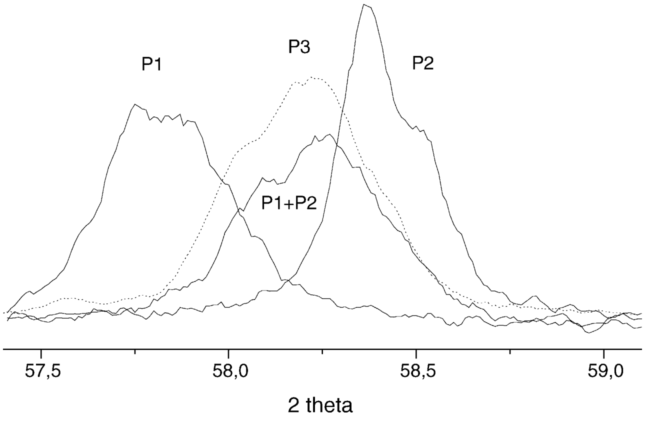

Fig. 4. XRD profiles of (2 1 1) peaks after sintering at 1573 K 6 min in air for perovskites: P1 = $La_{0.6}Sr_{0.2}Ca_{0.1}Bi_{0.1}Ga_{0.6}Mg_{0.1}Zn_{0.1}Fe_{0.2}O_{3-x}$; P2 = $La_{0.4}Ca_{0.4}Bi_{0.2}Mn_{0.6}Fe_{0.4}O_{3-x}$; P1 + P2 – nanocomposite; P3 – complex perovskite with chemical composition P1 + P2.

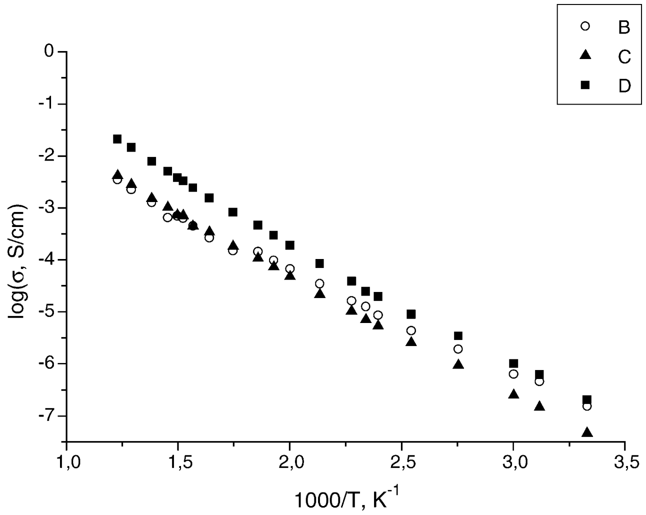

Fig. 5. Arrhenius plot of the total electrical conductivity in air of perovskite $P_{ion} = La_{0.6}Sr_{0.2}Ca_{0.1}Bi_{0.1}Ga_{0.6}Mg_{0.1}Zn_{0.1}Fe_{0.2}O_{3-x}$ (B) and composites 1:1 (C) and 3:1 (D) with electronic conductor $P_e = La_{0.4}Ca_{0.4}Bi_{0.2}Mn_{0.6}Fe_{0.4}O_{3-x}$.

The total conductivity in air of sintered ceramic disks comprised of individual complex oxides obtained by the mechanosynthesis and some composites is shown in Fig. 5. The decreased low temperature conductivity of composites with a ratio of 3:1 suggests interdiffusion during the sintering.

Typical curves for sample reduction by methane and oxygen desorption for the reoxidized Fe- and Co-containing composites are shown in Figs. 6 and 7. The ceria-based composite is not destroyed by a deep reduction down to metallic Fe, and Co and carbides thus form a rigid skeleton, which helps to maintain the mechanical integrity of the MIEC composite membrane. An estimation of the oxygen

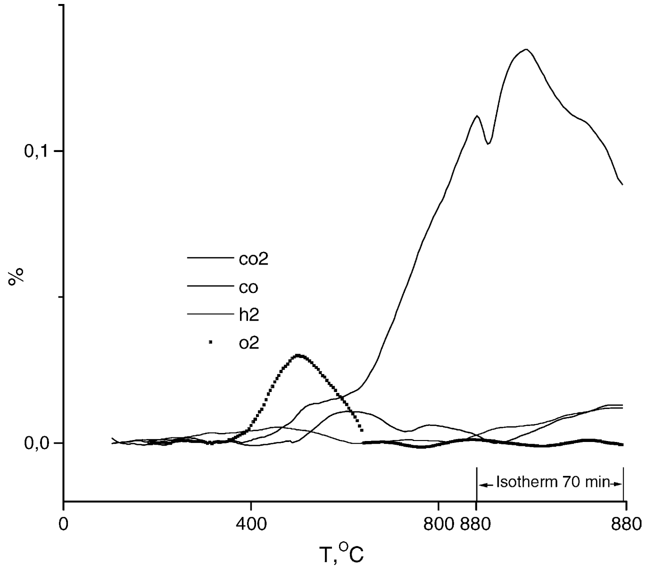

Fig. 6. Typical curves of CH_4 TPR – dependence of gas concentration in % on the temperature for F + P composite $Ce_{0.7}Pr_{0.3}O_{1.85} + Sr_{0.7}La_{0.2}Ba_{0.1}Fe_{0.5}Co_{0.5}O_{3-\delta}$.

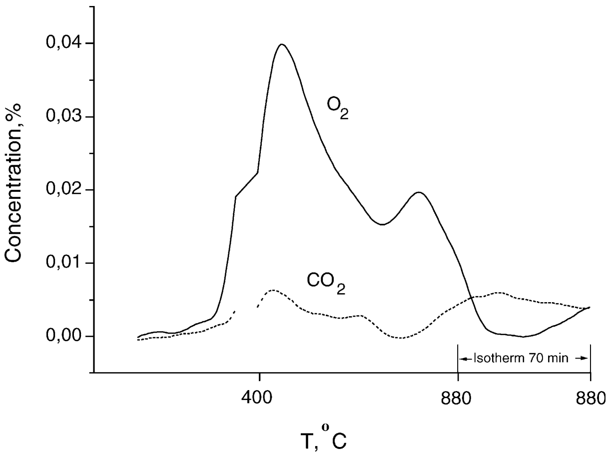

Fig. 7. Typical O_2 TPD curve for reoxidized F + P composite.

mobility made by using the maximum rate of reduction by methane gives a value ~10^{18} oxygen atoms/m^2s, which is of the same order as that found for the best materials by direct measurement of the oxygen permeability [7].

The optimal design of a membrane for methane conversion into syngas must consist of five layers [27]: (1) a macroporous support with a thickness ~1 mm of the MIEC conductor, which possesses a high rate constant of the surface exchange reaction and good mechanical properties; (2) an intermediate microporous layer; (3) a fully dense ceramic layer with a thickness ~10 μm of the MIEC conductor or the composite with a chemical composition close to that in layer 2; (4) a protecting thin layer of a composite based on gadolinium doped ceria and the $LaMnO_3$-based electronic conductor; (5) a finely dispersed catalyst for efficient partial oxidation of methane. Such a design of the membrane provides the stability against oxidizing and reducing atmospheres simultaneously, a high oxygen permeability due to the small thickness of the dense ceramic layer and a high rate constant of the oxygen exchange reaction, which usually limits the permeability of thin films [28]. The chemical compatibility of the layers in a membrane is very important to decrease the interdiffusion causing degradation of performance. Four-layered membranes without catalyst, which can be introduced by spray deposition in the last stage, were fabricated by consecutive operations of slurry casting and one stage sintering at a temperature of 1573 K for 6 min. SEM images of one membrane are shown in Fig. 8. The density of the ceramics measured in individual samples sintered at the same conditions is about 85, 90, 97 and 97% for layers 1–4 accordingly. The medium grain size is about 400 nm. The composition of the layers in the membrane presented in Fig. 8 is as follows:

(1) thickness ~1 mm, 90% of large agglomerates + 10% of aggregates (~1 μm) of the complex perovskite $P_e = La_{0.4}Ca_{0.3}Sr_{0.1}Bi_{0.1}Y_{0.1}Fe_{0.4}Mn_{0.3}Co_{0.2}Ni_{0.1}O_{3-x}$;

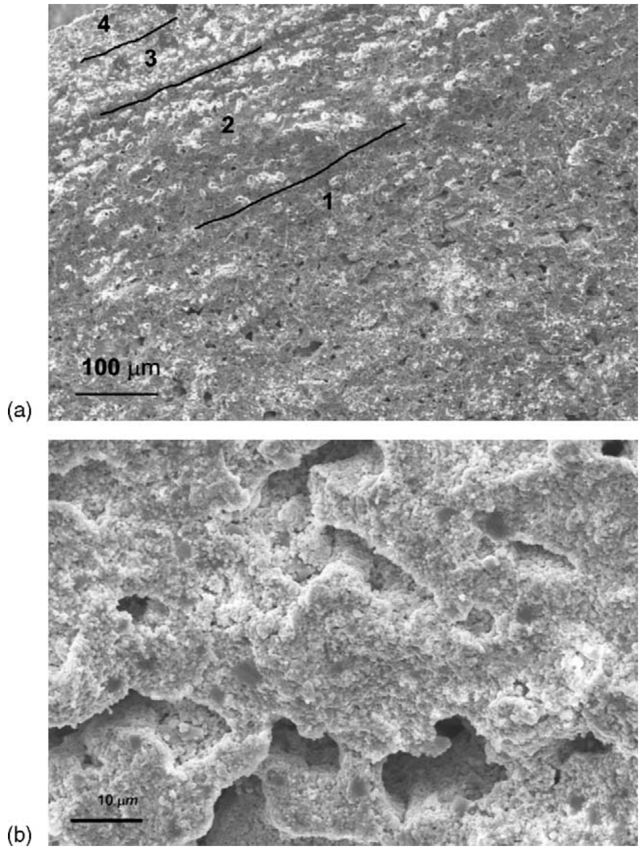

Fig. 8. (a) Cross-section view of four-layered membrane, (b) surface image of porous support – layer 1.

(2) thickness ~100 μm, 50% of medium (~10 μm) size agglomerates P_e + 50% of fine (~3 μm) agglomerates of the perovskite $P_{ion} = La_{0.6}Ca_{0.1}Sr_{0.2}Bi_{0.1}Ga_{0.6}Mg_{0.1}Zn_{0.1}Fe_{0.1}Co_{0.1}O_{3-x}$;

(3) thickness ~30 μm, nanocomposite $3P_{ion} + P_e$ from superfine (<1 μm) fractions of aggregates;

(4) thickness ~20 μm, nanocomposite $3F_{ion} + P_e$ (where $F_{ion} = Ce_{0.8}Gd_{0.2}O_{1.9}$, $P_e = La_{0.4}Sr_{0.3}Bi_{0.3}MnO_{3-x}$).

The mechanical integrity of a planar membrane is provided by close shrinkage of all layers during sintering. It is the main advantage of the proposed approach. The content of expensive elements in the ceramic layers 3–5 is small enough and gives a possibility of membrane recycling for the production of porous supports. The conventional deposition of nitrogen impermeable ceramic layers on the sintered porous substrate needs few consequent operations of spray deposition and sintering to close cracks [29].

In our opinion, a promising approach for the design of multilayer membranes should combine both mechanochemical and Pechini routes, each offering some advantages. Thus, the mechanochemical method provides large agglomerates for the porous substrate and compatible nanocomposites with a high green density and sintering activity, while the Pechini process produces a binding polymer and a catalyst precursor [22]. The usual thickness of protecting films derived by the Pechini process for one operation of deposition is ∼0.2 μm as compared to ∼20 μm produced by the casting of a slurry based on mechanochemical powders (cf. Fig. 8).

Measurements of permeability and catalytic efficiency of the developed multilayered membranes from the composites based on complex cubic perovskites and fluorites are currently in progress.

4. Conclusions

A new strategy for the development of multilayered membranes for methane conversion in CMR is proposed based on the application of the mechanochemical approach. The main advantages of the proposed strategy are as follows: superfast mechanosynthesis of complex perovskites and fluorites possessing a high green density and sintering activity at room temperature; possibility of production of compatible nanocomposites with MIEC properties; close shrinkage of different layers from the porous support to the dense ceramics; possibility of up-scaling by using a simple casting technology for the fabrication of planar and tubular multilayered membranes; possibility of membrane reutilization for the production of porous supports. An even more promising approach may include as well an application of the Pechini route for the deposition of protecting dense layers.

Acknowledgement

This work was supported by INTAS, grant 01-2162, and RFBR, 02-33330.

References

[1] Y. Teraoka, H.M. Zhang, S. Furukawa, N. Yamazoe, Chem. Lett. (1985) 1743.

[2] Y. Teraoka, T. Nobunaga, K. Okamoto, N. Miura, N. Yamazoe, Solid-Sate Ionics 48 (1991) 207.

[3] P.N. Dyer, R.E. Richards, S.L. Russek, D.M. Taylor, Solid-State Ionics 134 (2000) 21.

[4] Y. Lu, A.G. Dixon, W.R. Moser, Y.H. Ma, U. Balachandran, Catal. Today 56 (2000) 297.

[5] A. Sammels, M. Schwartz, R.A. Mackay, T. Barton, D. Peterson, Catal. Today 56 (2000) 325.

[6] H. Gleiter, Progr. Mater. Sci. 33 (1989) 223.

[7] H. Takamura, M. Kawai, K. Okumura, A. Kamegava, M. Okada, Mater. Res. Soc. Symp. Proc. 756 (2003) EE8.111.

[8] V.V. Kharton, A.V. Kovalevsky, A.P. Viskup, F.M. Figueiredo, A.A. Yaremchenko, E.N. Naumovich, F.M.B. Marques, J. Electrochem. Soc. 147 (2000) 2814.

[9] U. Nigge, H.-D. Wiemhofer, E.W.J. Romer, H.J. Bouwmeester, T.R. Schulte, Solid-State Ionics 146 (2002) 163.

[10] V.V. Zyryanov, N.F. Uvarov, V.G. Kostrovskii, V.A. Sadykov, T.G. Kuznetsova, V.A. Rogov, V.I. Zaikovskii, Y.V. Frolova, G.M. Alikina, G.S. Litvak, E.B. Burgina, E.M. Moroz, S. Neophytides, Mater. Res. Soc. Symp. Proc. 755 (2003) DD 6.27.1.

[11] J.K. Meen, O.A. Goksen, I.-C. Lin, K. Mukker, B. Nguyen, Mater. Res. Soc. Symp. Proc. 658 (2001) GG9.14.1-6.

[12] O.A. Goksen, J.K. Meen, A.J. Jacobson, D. Elthon, Mat. Res. Soc. Symp. Proc. 658 (2001) GG4.7.1-5.

[13] C. Li, T. Hu, H. Zhang, Y. Chen, J. Jin, N. Yang, J. Membr. Sci. 226 (2003) 1–7.

[14] V.V. Kharton, A.V. Kovalevsky, A.P. Viskup, A.L. Shaula, F.M. Figueiredo, E.N. Naumovich, F.M.B. Marques, Solid-State Ionics 160 (2003) 247.

[15] M. Mogensen, N.M. Sammes, G.A. Pompsett, Solid-State Ionics 129 (2000) 63.

[16] P. Knauth, H.L. Tuller, Solid-State Ionics 136–137 (2000) 1215.

[17] M.P. Pechini, US Patent 3,330,697 (1967).

[18] M. Schroeder, K.Q. Huang, H.Y. Yin, J.B. Goodenough, Proceedings of the International Symposium “Solid State Ionic Devices”, The Electrochemical Society Proceedings Series, PV 99-13, Pennington, NJ, 1999, pp. 121–130.

[19] V.V. Zyryanov, N.F. Uvarov, Inorg. Mater. 40 (7) (2004) 729.

[20] V. Zyryanov, N. Uvarov, V. Sadykov, G. Alikina, L. Ivashkevich, M. Ivanovskaya, S. Neophytides, Proceedings of the X APAM Topical Seminar “Nanoscience and Technology”, Novosibirsk, Russia, 2003, p. 173.

[21] V.V. Zyryanov, V.F. Sysoev, V.V. Boldyrev, T.V. Korosteleva, USSR Invention Certificate No. 1375328 (1988).

[22] V.A. Sadykov, N.N. Bulgakov, V.S. Muzykantov, et al. in: N. Orlovskaya, N. Browning (Eds.), Mixed Ionic Electronic Conducting Perovskites for Advanced Energy Systems, Kluwer Academic Publishers, Boston/Dordrecht/London, 2004, p. 49.

[23] V.V. Zyryanov, USSR Invention Certificate No. 1403439 (1988).

[24] V.V. Zyryanov, in: E.G. Avvakumov (Ed.), Mechanochemical Synthesis in Inorganic Chemistry, Nauka, Novosibirsk, 1991, p. 102.

[25] V.V. Zyryanov, Interceram 52 (1) (2003) 22.

[26] V.V. Zyryanov, Inorgan. Mater. 34 (12) (1998) 1525.

[27] V.V. Zyryanov, N.F. Uvarov, V.A. Sadykov, et al. Book of Abstracts of the Sixth International Conference on Catalysis in Membrane Reactors ICCMR-6, Lahnstein, Germany, July 6–9, 2004, p. 41.

[28] H.J.M. Bouwmeester, A.J. Burggraaf, in: P.J. Gellings, H.J.M. Bouwmeester (Eds.), CRC Handbook of Solid State Electrochemistry, CRC Press, 1997, p. 481.

[29] J.T. Ritchie, Thesis, University of Houston, USA, 2001.